UCRL-ID-133165

In-Situ Identification of Anti-Personnel Mines Using Acoustic Resonant Spectroscopy

Randy S. Roberts
Roger L. Perry

February 1999

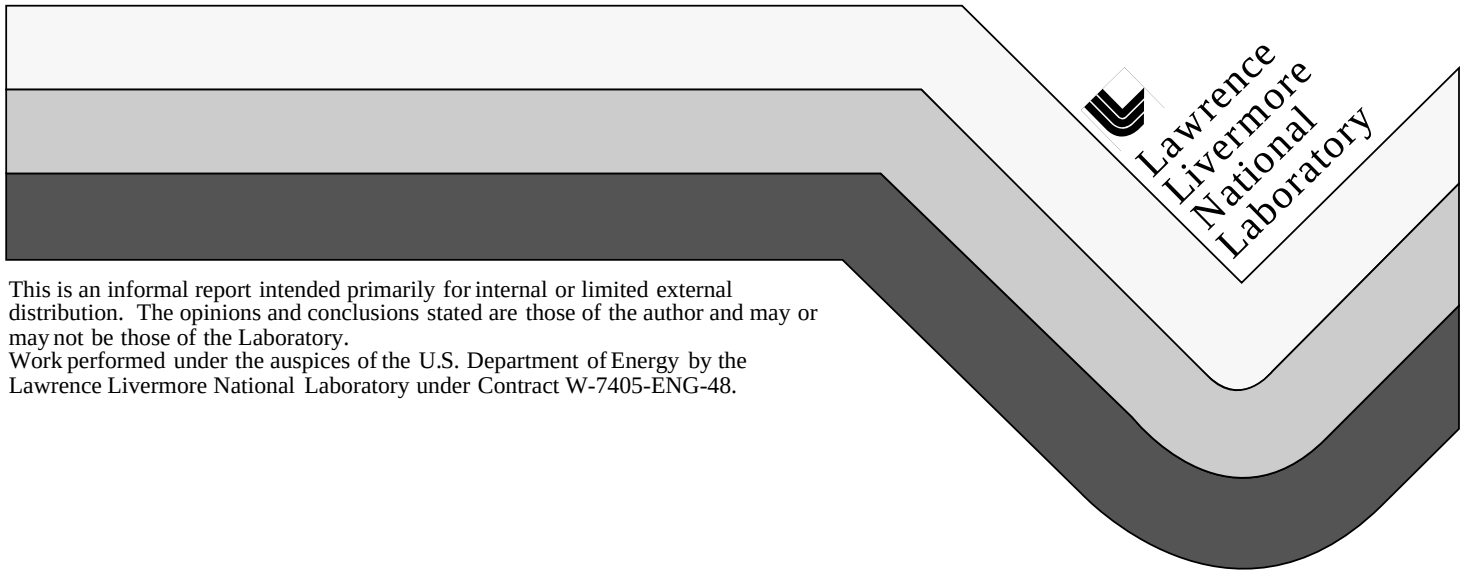

In-Situ Identification of Anti-Personnel Mines Using Acoustic Resonant Spectroscopy

Randy S. Roberts (DSED/EE and MMED/ME)
and Roger L. Perry (DSED/EE and MMED/ME)

Abstract

A new technique for identifying buried Anti-Personnel Mines is described, and a set of preliminary experiments designed to assess the feasibility of this technique is presented. Analysis of the experimental results indicates that the technique has potential, but additional work is required to bring the technique to fruition. In addition to the experimental results presented here, a technique used to characterize the sensor employed in the experiments is detailed.

1. Introduction

The detection of buried Anti-Personnel (AP) mines is a problem of tremendous importance in many parts of the world. The International Committee of the Red Cross and Red Crescent Societies estimates that approximately 110 million AP mines have been placed in 64 countries world wide [1]. The disruption to daily life caused by AP mines in these countries is enormous. As an example, over the last fifteen years land mines in Afghanistan have caused 600,000 casualties (one out of fifty Afghans), one third of which are women and children. In addition to producing direct injuries, land mines often contribute to the malnutrition and promote disease in a population. For example, safe drinking water can be denied to a village with the mere suspicion of a land mine field. The village might respond by using unsafe supplies thereby increasing the risk of dysentery. Similarly, land mines can easily remove farmland from production, thereby increasing the risk of malnutrition.

Modern AP mines are surprisingly simple, effective and insidious devices. They tend to be cylindrical in shape, with diameters ranging from 6 to 15 cm, and heights from 3 to 6 cm [2]. They often have simple pressure sensitive triggers, requiring a mass of 3 to 25 kg for detonation. The explosive charge is typically 50 to 200 gm of TNT. This amount of explosive tends to cause serious injury to an adult, e.g., destroy a foot or leg, and kill small children. Modern mines contain very little metal, and thus are very difficult to locate with conventional metal detection instruments. Operationally, they are buried in soil to a depth of 1 to 4 cm and laid out in a variety of patterns, depending on the application. They are very robust devices, and can remain operational for decades after planting.

Conventional demining techniques are time consuming, labor intensive and dangerous. Due to its thoroughness and effectiveness against minimum-metal mines, manual probing is the most widely used demining technique in the world [3]. In this technique, a deminer pushes a probe into the ground at a shallow angle. The probe is lifted slightly and extracted. A deminer trained in this technique can feel a mine above the probe as it is lifted and extracted. To insure that all AP mines in an area are detected, probing is performed over a 3 cm by 3 cm grid. With this type of search pattern, one deminer can clear approximately one square meter of land per day.

Emerging mine detection techniques include infrared sensing for wide area detection, olfactory and chemical sensors for explosive detection, and ground-penetrating radar for detecting buried objects. Of these techniques, ground-penetrating radar has shown the most promise for demining. Indeed, a current project at LLNL seeks to image buried objects using the Micropower Impulse Radar (MIR) as an imaging sensor. The idea is to rapidly survey the top layer of soil for objects that have geometric properties similar to AP mines. When such an object is detected, it is marked for probing. The application of such a ground imaging system would no doubt increase the efficiency of deminers. However, deminers could easily be inundated by the large number of false alarms produced by shrapnel, debris and other objects that produce images similar to AP mines.

2. *In Situ* AP Mine Identification Technique

The technique described here allows a deminer to discriminate between mines and other buried objects *in situ*. It thus provides a means to distinguish AP mines from other buried objects detected by ground imaging systems. The technique is based on acoustic resonance spectroscopy (ARS), a technology that has been successfully applied to the identification of chemical munitions [4-6]. The ARS technique is based on the premise that objects of interest (such as AP mines) have characteristic resonant frequencies that we can excite, detect and are nominally reproducible. Since the resonant frequencies of an object are functions of the object's geometry and materials of construction, it follows that objects of a similar nature will have similar patterns of resonant frequencies. Thus, the frequency response pattern of an object can be used to identify it. As previously mentioned, this technique was used with great success in the Acoustic Resonant Spectroscopy (ARS) Munition Classification System (MCS) developed at LANL. An instrument based on this concept was developed, tested, and accepted for use as a verification tool for the Chemical Weapons Convention.

There are several ways to estimate the acoustic resonance spectrum of an object. In the case of an AP mine, the objective is to obtain the spectrum in the most non-invasive manner possible. (See Figure 1 for a schematic diagram of the technique.) To begin with, an excitation force spanning the frequency band containing the resonances is applied to (or near to) the object. The magnitude of the excitation force does not need to be large to obtain a useful spectrum. (In the case of the ARS-MCS, a piezoelectric transducer provides the excitation force. The induced vibrations on the munition have amplitudes on the order of 10 nm.) For AP mines, a simple approach is to touch the object with a probe that produces low amplitude vibrations over the frequency band of interest. Although this requires touching the object, it is perhaps the best way to excite the object's resonant frequencies. And as previously noted, touching mines with a probe is accepted practice with deminers. With regards to the form of excitation signal, a narrow-band sinusoid stepped over the frequency range of interest has a major benefit: the tone provides a coherent reference for processing the received signal. A coherent reference can be used to increase the signal-to-noise ratio of the returned signal, and can also be used to extract phase information.

In order to collect the frequency response of the object, a sensor is required to detect the object's vibrations. In general, radar is well suited for the non-invasive sensing of vibrations. In particular, the MIR technology invented at LLNL provides a unique means of non-contact, standoff vibration sensing [7]. Even though the objects of interest are buried, the burial depths are shallow enough that a low-power radar should have little problem sensing the vibrations. By using localization information provided by the LLNL MIR ground imaging radar, the range gate and other parameters on the vibration sensing radar can be adjusted to maximize the signal-to-noise ratio of the returned signal.

2.1 Experimental Results

We have conducted several experiments to assess the feasibility of the identification technique. The experiments consisted of measuring the acoustic resonant spectrum of several objects over a limited frequency range. The measurements were collected with unburied objects to maximize the signal-to-noise ratio. Four objects of similar geometry were used in the experiments (cf. Figure 2). The first object was an M14 mine (inert); the second a nondescript mine detection target (MDT); and the third object serving as debris was a galvanized nipple covered with duct tape. A fourth object, not pictured, which also served as debris was a plastic can containing putty. The M14 surrogate is made of a hard plastic, roughly cylindrical in shape and approximately 4.3 cm in height, and 5.2 cm in diameter. The MDT is also made of hard plastic, and is approximately 3.5 cm in height, and has a diameter of 7.5 cm. The pipe is 8 cm in height and has a diameter of 6 cm, and the putty-filled plastic can has a diameter of approximately 6.1 cm and height of 8 cm. The objects were secured in a wooden cradle for the experiments. An HP35670A signal generator provided the excitation signal for the experiments. That signal was amplified and applied to a Wilcoxan F4 vibrator. A probe approximately one foot in length was attached to the vibrator, and touched to the sides of the objects. See Figure 3 for a picture of the experimental arrangement. Object vibrations were sensed by a low power MIR borrowed from the speech analysis laboratory. The radar was placed 60 mm from the surfaces of the objects, in an orientation perpendicular to the surface. Both the drive signal from the HP generator and the return signal from the MIR were digitized at a 40 kHz sampling rate.

In the first experiment, spectra from the objects were collected over the frequency ranges of 50 to 100 Hz, 100 to 200 Hz, and 200 to 400 Hz. In each band, the frequency of the drive signal was stepped over approximately thirty tones, each with a duration of 1.5 seconds. The response signals from the radar were resampled to 10 kHz, normalized to the maximum amplitude of the excitation signal, and Fourier transformed. Magnitude plots of the frequency responses in the 200 to 400 Hz excitation band are shown in Figure 4. The upper plot (blue) is the response of the M14 AP mine, the middle plot (red) the response of the MDT, and the bottom plot (green) the response of the pipe. Notice that the three objects produce distinguishable spectra over this frequency range. The M14 produces a large response in the 325 to 400 Hz region whereas the responses of the other two objects are much more subdued. In contrast, the 275 to 325 Hz band of the M14 is slightly depressed compared to the same band in the other objects. The responses in the 200 to 275 Hz band are somewhat similar in that they all tend to increase as the frequency increases from 200 to 250 Hz. The mine surrogate and the pipe have similar responses in the 275 to 400 Hz bands with a noticeable spike in the pipe's response at 275 Hz, and null at the same frequency in the mine surrogate. The other frequency ranges contained similar spectral features. As an aside, spectra from the can of putty is uninteresting—it contains few spectral features. Lack of features in the putty spectra is not unusual since putty and its plastic container are non-rigid. Most of the excitation energy is absorbed by the putty, leaving little response signal.

A second set of experiments was performed to assess the variability of the spectral measurements. These experiments consisted of multiple measurements of the response of the objects to a sinusoidal excitation over a band of 200 Hz to approximately 500 Hz. The data for these experiments were collected in a manner similar to the previous experiment. Raster plots of the resulting spectra are shown in Figures 5 through 8. Spectra from the MDT and pipe, as illustrated in Figures 5 and 6, show some degree of consistency over the ensemble of measurements. (The large spikes in the spectra are a result of the vibrator attempting to maintain a constant force on the objects as the frequency increases. The spikes occur somewhat randomly throughout the spectra, but are readily discernable.) For

example, the MDT tends to have a larger response in the region of 250 to 275 Hz than in the region of 200 to 250 Hz. Similarly, the pipe has a response that appears to decrease from 200 to say 240 Hz, and then tends to increase from 240 to 275 Hz. For both objects, the response beyond 300 Hz appears flat. Evaluation of the response of the M14 and the putty-filled can, illustrated in Figures 7 and 8, is more difficult. The spectra of both objects appear dominated by noise. However, the spectra of the M14 seem to have some structure in the region of 300 to 400 Hz where the putty does not. But again, firm conclusions are difficult to draw due to the lack of sufficient response from the excitation signal. In summary, the spectra of the MDT and the pipe appear similar in repeated measurements. Due to the lack of signal, the variability of the spectra of the M14 and putty filled can not be accurately assessed.

2.2 Conclusions and Observations

Although our preliminary experiments indicated the feasibility of this approach to AP mine identification, several critical issues remain. These issues include the structure of the resonant spectra of AP mines (and similar objects) in the frequency range above 1 kHz, the variability of the resonant spectra in this region and collecting spectra from buried objects. We estimate that the resonant frequencies of the M14 mine and MDT occur at approximately 1.2, 4.8, 10.8, ..., kilohertz [8]. A similar set of resonant frequencies occurs for the pipe and putty-filled can. The vibrator used in the experiments has a frequency range of 10 Hz to 7.5 kHz, so it can reach into the frequency band of interest. Other vibrators are available that can extend the upper limit of the excitation frequency to 20 kHz. However, the radar employed in the experiments has an upper frequency limit of approximately 1 kHz. As a result, we were unable to investigate the region above 1 kHz where potentially unique information about AP mines (i.e., their resonant peaks) is located. The frequency limit of our radar imposed a severe constraint on the search for spectral features.

Concerning spectral variability, robust discrimination algorithms depend on spectral features that can be reliably extracted from resonant spectra. The greater the variability of the resonant spectra, the less reliable the spectral features and thus poor discrimination. We collected some data to assess spectral variability, but the results were disappointing. In particular, good signal-to-noise ratios were difficult to obtain. Two candidates emerged as the source of this problem: coupling energy into the objects and the radar. Coupling energy from the vibrator into the objects could be improved by developing a specialized tip for the probe. Such a tip might allow for more efficient transfer of energy. Issues involving the radar are described in the sequel. Finally, although our experiments have laid the groundwork for this identification technique, the measurement of spectra from buried objects remains to be performed. This set of experiments would collect spectra from objects similar to the ones used here, but buried in a variety of soils (sand, rock, clay, etc.) and under a variety of conditions (dry to very wet).

We conclude this section with some thoughts on the automated pattern classification of spectra. Automated pattern classification is necessary to provide deminers with confidence in the technique. From the deminer's point of view, the processing should produce a binary decision ("Yes, the object is a mine," or "No the object is not a mine"), along with a numerical measure of confidence. The key to providing such a decision to the deminer resides in the object's spectral features. (Spectral features are quantities that can be extracted from spectra that are useful for distinguishing one class of spectra from another.) If invariant spectral features can be found, clustering techniques can be used for classification. Such was the case in the ARS-MCS liquid-solid discrimination algorithm where features extracted from the spectra of liquid and solid-filled munitions grouped into

two clusters, one for solids, and one for liquids. If the spectral features tend to be variable (due to soil conditions, age of mine, etc.), a comparative approach can be employed. Such was the case in the ARS-MCS munition classification algorithm where spectral features of different chemical munitions (in this case the frequencies of resonant peaks) tended to vary. The munition classification algorithm compared spectral features from the unknown munition to templates of spectral features built from known munitions. (The templates quantified the variability of the spectral features.) While the algorithms developed for the ARS-MCS may not be directly applicable to the proposed project, they form a strong foundation for future algorithm development.

3. MIR Frequency Characterization

The frequency characteristics of the MIR employed as a vibration sensor for this project are not well understood. As an expansion of the scope of the project, an effort was undertaken to characterize the sensor. Characterization consisted of attempting to estimate the response of the MIR to a known displacement over a range of frequencies. To perform the characterization, a large shaker in the Modal Analysis Laboratory was used as the excitation source. The shaker, fitted with a target, was programmed to sweep through a range of frequencies, and the responding voltage from the MIR was recorded. To determine the precise motion of the target, two techniques were employed: a Linear Variable Differential Transformer (LVDT) and an accelerometer. The attractiveness of the LVDT is that it measures displacement directly. The accelerometer measures displacement indirectly by appropriately integrating its output twice. Details of the characterization procedure and results are presented below and in [9]. However, before discussion characterization results, issues regarding use of the LVDT and accelerometer to determine the displacement of the target are first described.

A Linear Variable Differential Transformer (LVDT) measures displacement directly. An LVDT is an electromechanical transducer that converts the linear motion of an object attached to it into a voltage. Essentially, it consists of a one primary coil and two secondary coils in a housing and a high-permeability core. As the object moves, the core (attached to the object) moves in and out of the coil housing (held stationary above the object). By applying an alternating current to the primary coil, the motion of the core through the housing is found as the differential AC voltage across the secondary coils.

The LVDT used in these experiments was a Macro Sensors PR 750-050 LVDT along with a DCM-1000 signal conditioning board. This particular sensor can measure linear displacement within ±0.050 inches. It has a sensitivity of 6.5 mV/V/mil (mV of output per V of excitation per .001 in. of core displacement). The DCM-1000 provides 3V of drive, and with a maximum travel of 50 mils, the maximum output of the LVDT is 0.975 V. For calibration, a shorting wire is temporarily connected across the output of the LVDT and the zero potentiometer adjusted for 0 volts output. The shorting wire is then removed, and the core placed in the LVDT body and physically moved to obtain an output voltage of 0. The core was then moved 0.050 inches using a dial caliper and the span control was adjusted for an output voltage of 10.0 volts. This procedure ensures that during data collection, each mil of travel of the LVDT core results in a voltage change of 200 mV.

In contrast to LVDTs, accelerometers measure displacement indirectly. Given a sinusoidal excitation, the displacement is found from acceleration by the equation

$$d = 9.807e3(a/4\pi^2 f^2)$$

where d is displacement in millimeters, a is acceleration in g's, and f is the frequency. This equation is derived by integrating a sinusoidal acceleration twice. The accelerometer used for the experiments was a Dytran Model 3134A (SN 243) accelerometer. Extensive documentation provided with the accelerometer detailed the sensor's calibration

The rig used to characterize the MIR sensor is illustrated in Figures 9 and 10. It consists of a large shaker with a target (a 6in x 6in aluminum plate) attached to the top, and a frame surrounding the shaker built from Klinger Rails. Two threaded holes were drilled into the plate, one to mount the accelerometer, and one to mount the core of the LVDT. The body of the LVDT was mounted to the frame and oriented so that an upward movement of the shaker plate would result in a positive voltage.

3.1 Experimental Results

A number of experiments were conducted to measure the response of the MIR to the motion of the target on the shaker. These experiments were conducted over the intersections of the pass bands of the sensor and shaker, which is on the order of 20 Hz to 300 Hz. The radar was positioned at the heights of 20 mm above the target and 60 mm above the target for the experiments. The results of the experiments are summarized in Figures 11 to 15. Figures 11 and 12 show exemplar plots of the responses of the LVDT, accelerometer and MIR (at a distance of 60 mm from the target) at 25 and 300 Hz. The units on the vertical scales of these plots vary depending on the quantity measured. In the case of the LVDT (the blue trace) and the accelerometer (green trace), the units are millimeters of displacement. For the radar, (the red trace), the units are tenths of volts. As previously noted, displacement is directly obtained from the LVDT, and indirectly from the accelerometer.

Study of Figures 11 and 12 reveal several interesting aspects of the signals. In particular, distortion appears in the MIR response signal at 300 Hz (cf. Figure 12). This distortion is particularly apparent near the peaks and troughs of the sinusoid, but is also visible elsewhere. Of greater concern is the relationship between the LVDT signal and the accelerometer signal as the frequency increases from 25 Hz to 300 Hz (cf. Figures 11 and 12). Observe that the displacement reported by the LVDT and computed from the accelerometer match rather well at 25 Hz, but differ as the frequency increases to 300 Hz. As the frequency increases, the displacement as computed from the accelerometer is less than that reported by the LVDT. Moreover, the phase of the displacement as computed from the accelerometer begins to lag the phase of the displacement reported by the LVDT. This is a rather troubling observation, as the LVDT is alleged to provide an accurate measure of displacement. Recall that for proper characterization of the MIR, the motion of the target must be accurately determined.

The pedigree of the accelerometer is extensive and well documented. It is beyond reproach. On the other hand, investigation of the LVDT revealed it as the most likely problem. A representative of Macro Sensors assures that the combination purchased would have no appreciable phase shift in the frequencies from 20 to 300 Hz, but a quick check on the bench seemed to disagree. Further investigation revealed that the conditioning board from Macro Sensors contained two low pass filters. Macro Sensors suggested eliminating one of the low pass filters via board modification. After performing these changes, a quick test shows the phase shift had been reduced substantially, but not completely. Alas, the LVDT as provided by Macro Sensors did not appear to be suitable for characterizing the MIR sensor. Further work in the area of the LVDT characterization is necessary if it is to be a viable tool in characterization of these radars.

As a result of the fiasco with the LVDT, the MIR sensor was characterized using the accelerometer to estimate target motion. The magnitude of the displacement of the target, over the frequency band of 20 to 300 Hz, is shown in Figure 13. Predictably, the magnitude of the target displacement appears as a low-pass function. Figures 14 and 15 show the (normalized) magnitude and phase of the MIR output in response to the target motion. The plots illustrate the responses of the MIR positioned 20 and 60 mm above the target. The magnitudes were determined by estimating the average amplitude of the envelope of the sinusoidal excitation and response signals for each frequency over the range of interest. In turn, the envelopes of the sinusoidal excitation and response signals were found using a Hilbert transform technique. The phase response was estimated using a zero-crossing procedure with the shaker motion used as a reference. Note that the magnitude response, shown in Figure 14 has been normalized to one millimeter of displacement. Normalization of the magnitude response can be troublesome, particularly for low signal-to-noise ratios. But for these data, the signal-to-noise ratio appeared adequate to perform the normalization.

The magnitude plots shown in Figure 14 reveal interesting behavior of the MIR sensor. The response at the 20 mm position has a gradual slope from ~0.1V/mm at 20 Hz to ~0.75V/mm at 300 Hz. At ~60 Hz and ~270 Hz, the magnitude is seen to jump from the baseline. These jumps are also observed in the phase plots of Figure 15, particularly at ~270 Hz. In contrast, the magnitude response of the MIR sensor at the 60 mm position exhibits a low pass characteristic with wide deviations occurring throughout the band. The normalized magnitude response at this position is also considerably larger than the response at the 20 mm position. The phase responses at the 20 mm and 60 mm positions, as illustrated in Figure 15, have similar characteristics. Both lag the motion of the shaker at 20 Hz, and decrease the lag as the frequency increases. The rate of decrease in lag is greater in the 20 to 100 Hz band, and becomes more gradual in the 150 to 300 Hz band. The characterization of the MIR at these positions provides some insight into the device, but additional characterization at other positions is necessary for a fuller understanding.

As a final note, one experiment was conducted to assess the sensitivity of the MIR sensor. The shaker was set to vibrate at 100 Hz with a 4.18 μm peak displacement. The MIR produced an output of 48.8 mV peak amplitude at a distance of 40 mm.

4. Summary

A novel technique for discriminating AP mines from other buried objects has been presented. The technique is based on measuring the acoustic resonant spectrum of a buried object using a probe to provide an excitation signal and a standoff radar to sense the object's response. Several experiments were performed on mine-like objects to assess the potential of the identification technique. One set of experiments found spectral features that might be used as the basis for discrimination algorithms. The second set of experiments indicates that the spectra of the object's have a tolerable degree of variability. Further research to identify spectral features in larger frequency bands, assess the variability of these features, and collection of spectra from buried objects is required to bring this technique to fruition.

A technique to characterize the frequency response of MIR sensors to mechanical vibrations was explored. The technique used a large shaker fitted with a target as an excitation source, and an accelerometer attached to the target to measure the displacement of the target. Magnitude and phase plots of the MIR used in this project (and used for speech research) were obtained over a frequency band of 20 to 300 Hz, and at standoff distances

of 20 and 60 mm. The plots reveal interesting behavior in the MIR sensor, but additional experimentation is required to develop a full understanding of the device.

5. Acknowledgments

The authors would like to thank John Holzrichter for suggesting the identification technique described in this report . They would also like to thank John and Greg Burnett for the use of their MIR and data acquisition system, and Tom Woehrle for the use of equipment in the Modal Analysis Laboratory. This project was supported by Engineering NDE Thrust Area and LDRD funding. This work was performed under the auspices of the U. S. Department of Energy by Lawrence Livermore National Laboratory under Contract W-7405-Eng-48.

6. Notes and References

[1] U.S. Army Communications Electronics Command, Night Vision and Electronic Sensors Directorate, Countermine Division, *Humanitarian Demining*, 1998. http://www.demining.brtrc.com. Also see *Direct and Indirect Consequences of Land Mines on Public Health*, http://www.demining.brtrc.com/contents.htm

[2] *Jane's Mines and Mine Clearing*, Colin King, ed., Jane's Information Group Inc., Alexandria, VA, 1997.

[3] We draw a distinction between humanitarian demining and mine field clearing. Mine field clearing refers to a military unit breaching a minefield. Often, this is accomplished by a simple linear path through the field. Speed is of the essence; safety and thoroughness of mine removal are secondary. In contrast, humanitarian demining calls for clearing large areas of terrain, thoroughness of mine removal is paramount (as is the safety of the demining crew), and speed is a secondary concern.

[4] R. S. Roberts, J. T. Chen, O. A. Vela and P. S. Lewis, "Munition Classification Using an Acoustic Resonance Spectroscopic Technique," *Proceedings of the Twenty-Seventh Annual Asilomar Conference on Signals, Systems, and Computers*, Pacific Grove, CA Nov 1-3 1993.

[5] R. S. Roberts, P. S. Lewis, J. T. Chen, and O. A. Vela, "Techniques for Classifying Acoustic Resonant Spectra," *Proceedings of the Twenty-Eighth Annual Asilomar Conference on Signals, Systems, and Computers*, Pacific Grove, CA Oct 30 - Nov 2, 1994.

[6] R. S. Roberts, P. S. Lewis, and O. A. Vela, "A Pattern Recognition Algorithm for the Blind Discrimination of Liquid and Solid filled Munitions," *Proceedings of the Twenty-Ninth Annual Asilomar Conference on Signals, Systems, and Computers*, Pacific Grove, CA Oct 29 - Nov 1, 1995.

[7] J. F. Holzrichter, G. S. Burnett, L. C. Ng and W. A. Lea, "Speech Articulator Measurements using Low Power EM-wave Sensors", *J. Acoustic Society Am.* 103 (1) 622, Jan 1998.

[8] E. Skudrzyk, *Simple and Complex Vibratory Systems*, Pennsylvania State University Press, University Park, 1966.

[9] R. Perry, Internal Memorandum, October 1998.

Figures

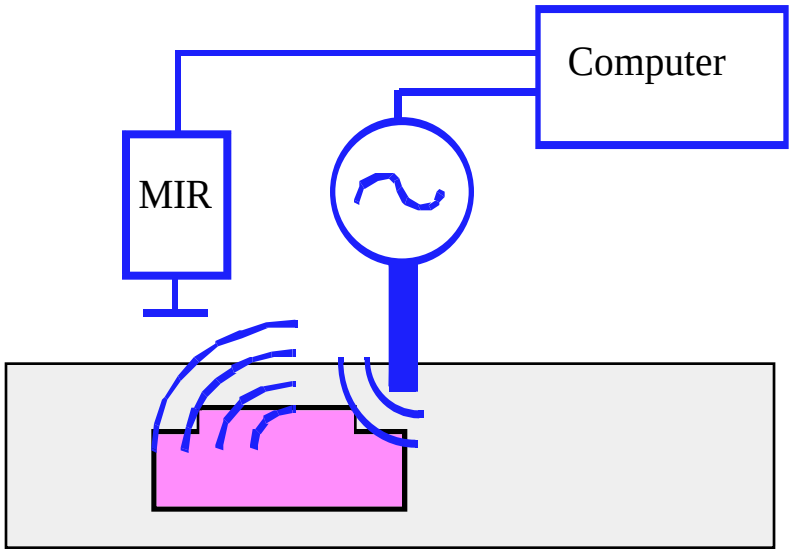

Figure 1: Schematic of the in-situ Anti-Personnel mine identification technique. A probe excites the buried object with a stepped frequency sinusoidal signal. The response of the object is received by a Micropower Impulse Radar, analyzed and classified by the computer.

Figure 2: Objects used in the Preliminary Experiments (the can of PlayDough is not shown). On the left is a M14 mine (inert), in the center is a nondescript Mine Detection Target (MDT), and on the right is a nipple covered in duct tape.

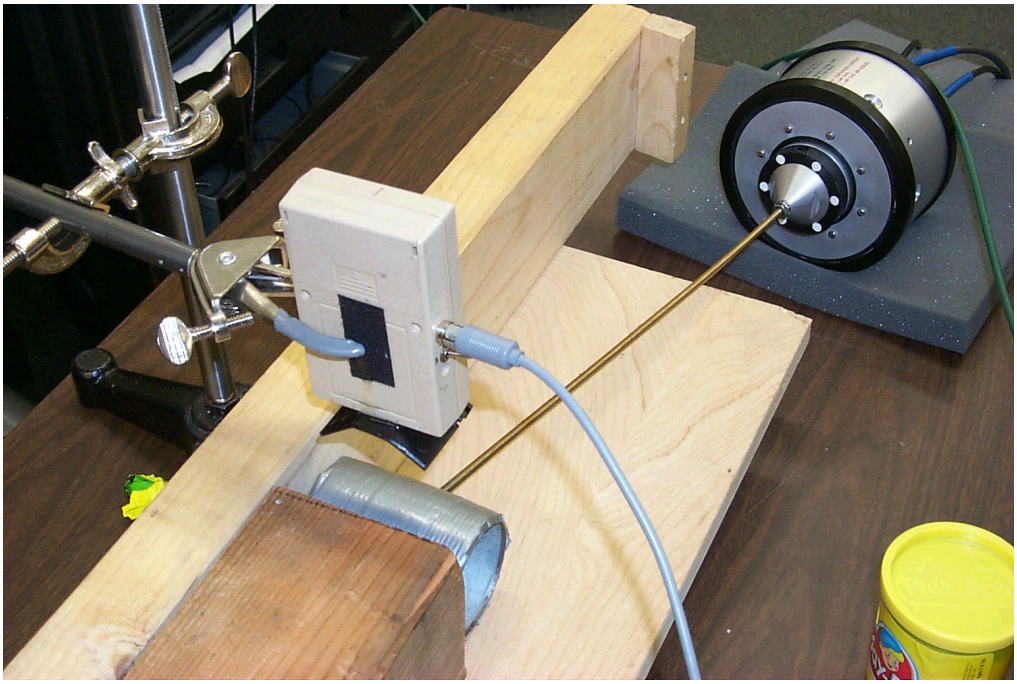

Figure 3: Experimental apparatus used to measure the acoustic resonant spectrum of surrogate mines and debris. The object under inspection is a small pipe covered with duct tape. The MIR radar (above the pipe) is typically used for speech analysis.

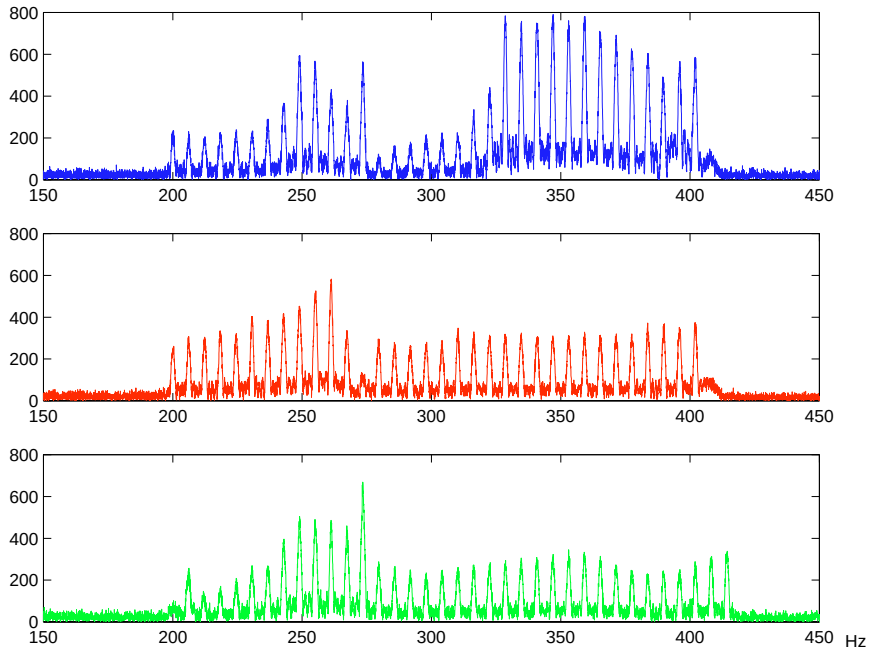

Figure 4: Magnitude response of the M14 (blue), MDT (red) and pipe (green).

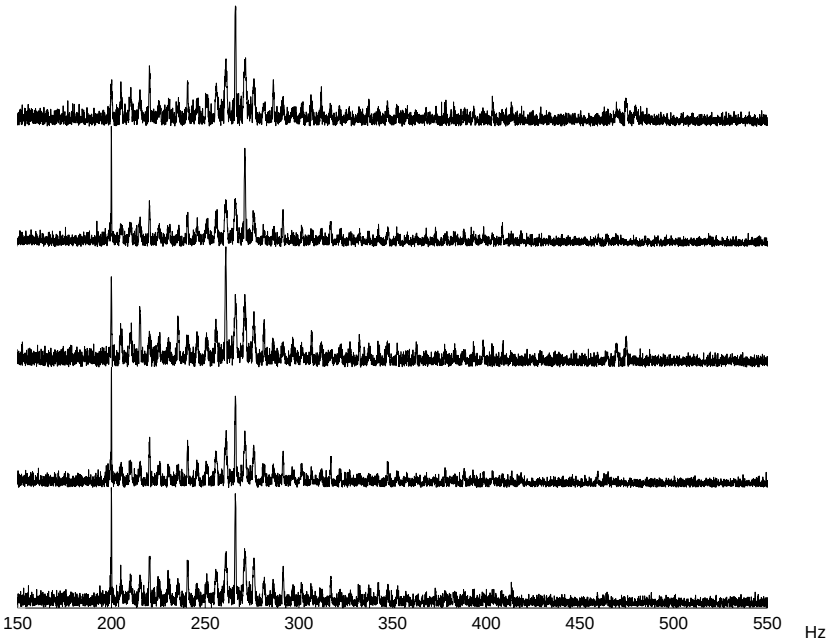

Figure 5: Ensemble of magnitude responses of the MDT.

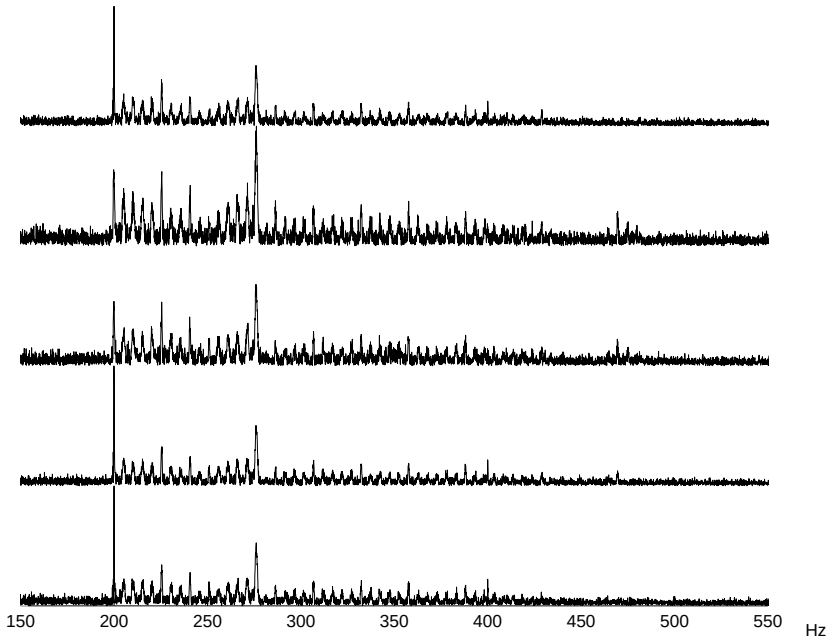

Figure 6: Ensemble of magnitude response of the duct-taped pipe.

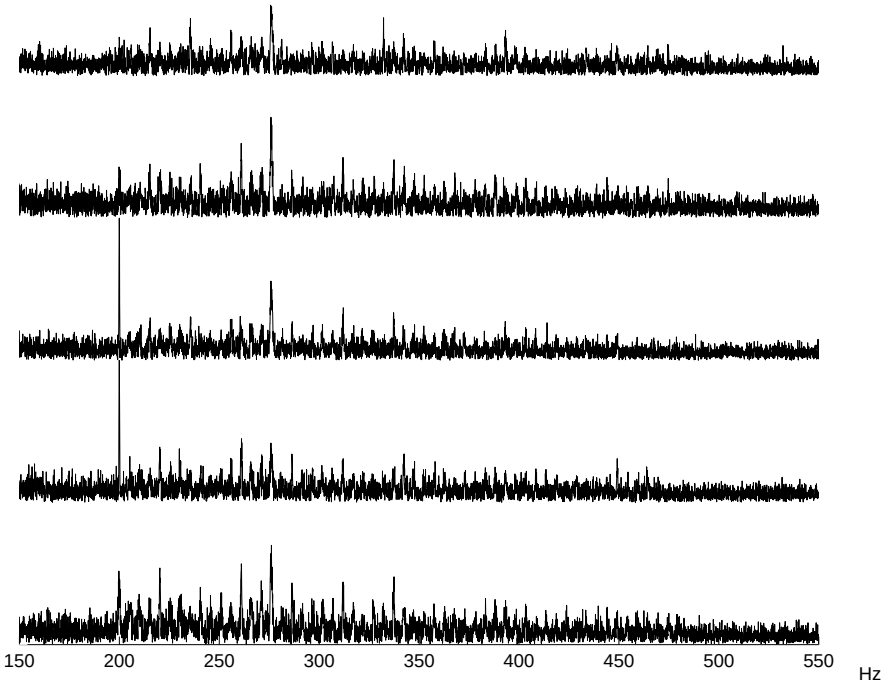

Figure 7 : Ensemble of magnitude response of the mine surrogate

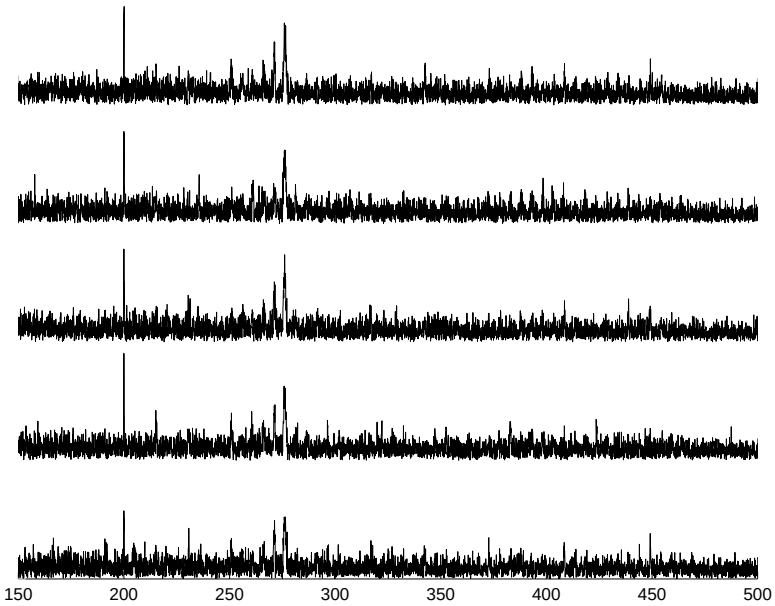

Figure 8: Ensemble of magnitude response of the putty-filled can.

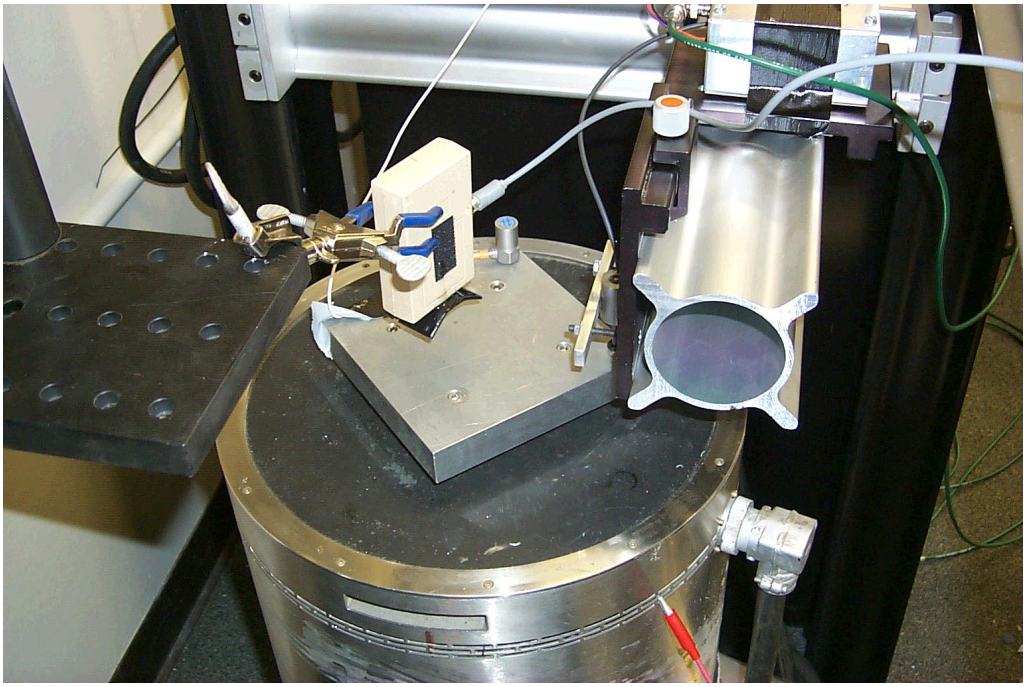

Figure 9: Close up view of the experimental arrangement used to characterize the radar. The radar illuminates the large aluminum plate, to which an accelerometer is mounted on the top corner of the target. The LVDT is also present, but not visible.

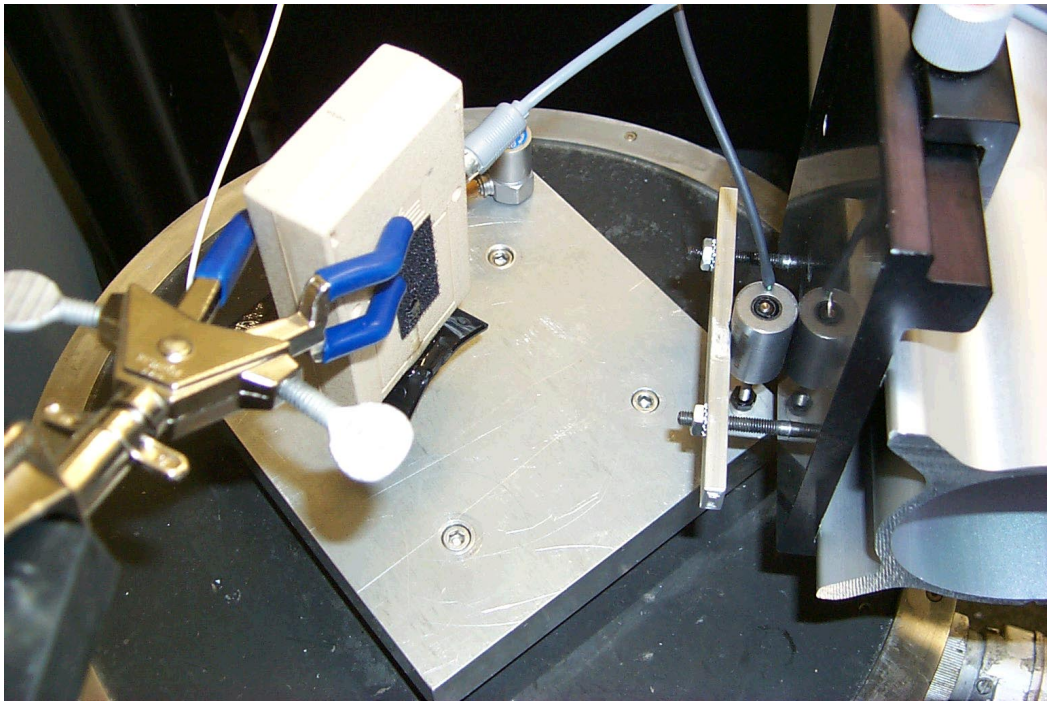

Figure 10: Close up view of experimental arrangement used to characterize the MIR sensor. The accelerometer is on the top corner of the target, and the LVDT is on the right corner.

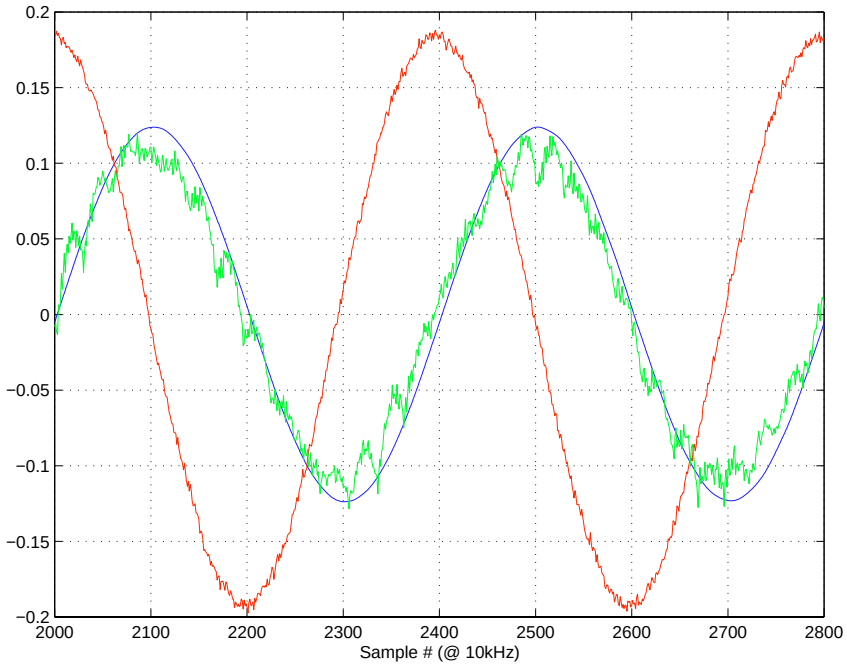

Figure 11: Plot of outputs of the radar at 60 mm from the target (red, voltage), the LVDT (blue, mm displacement) and the accelerometer (green, mm displacement) at 25 Hz.

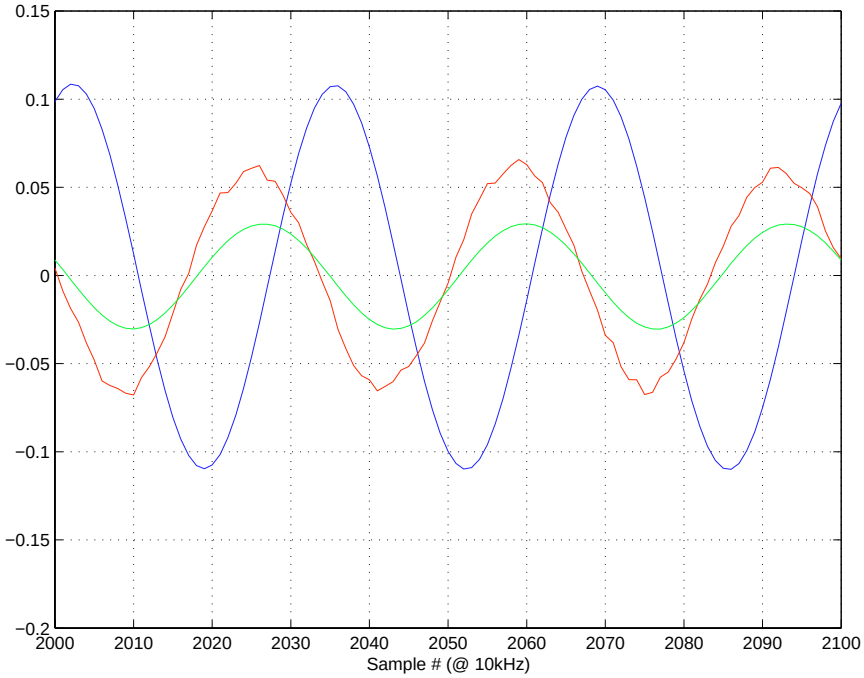

Figure 12: Plot of outputs of the radar at 60 mm from the target (red, voltage), the LVDT (blue, mm displacement) and the accelerometer (green, mm displacement) at 300 Hz.

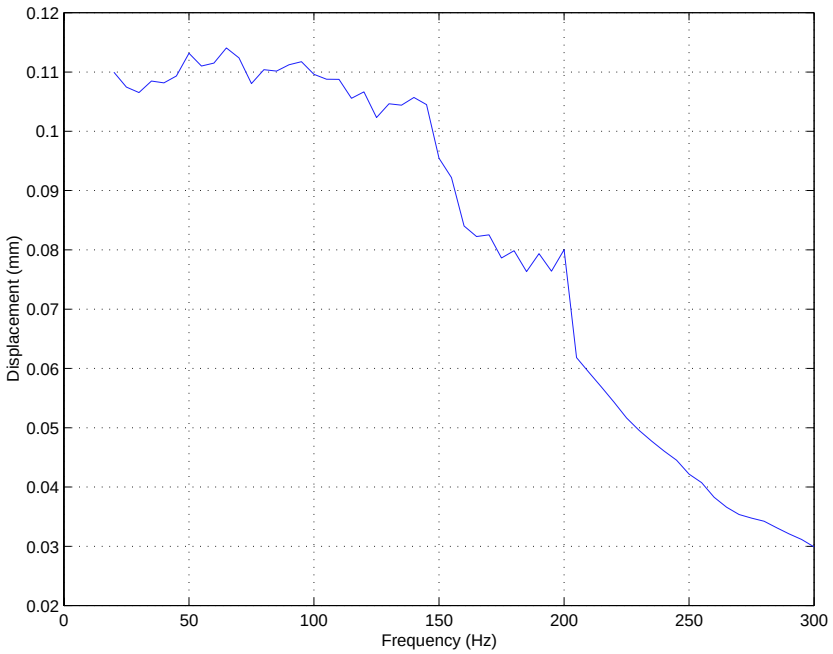

Figure 13: Plot of displacement of target (in millimeters) using an accelerometer to measure displacement.

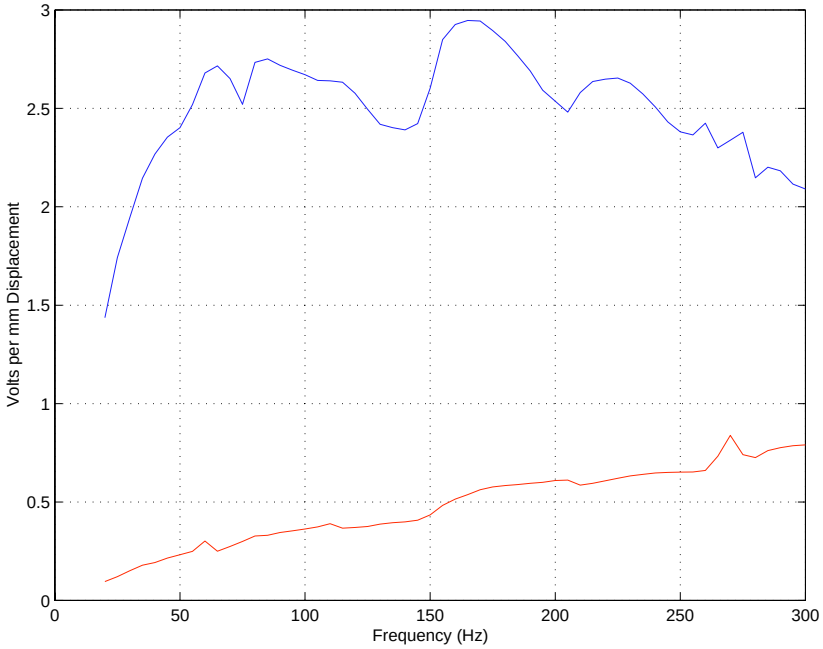

Figure 14: Magnitude plots of the output of the MIR when positioned 60 mm (blue) and 20 mm (red) above the target. The magnitude is normalized to 1mm of target displacement.

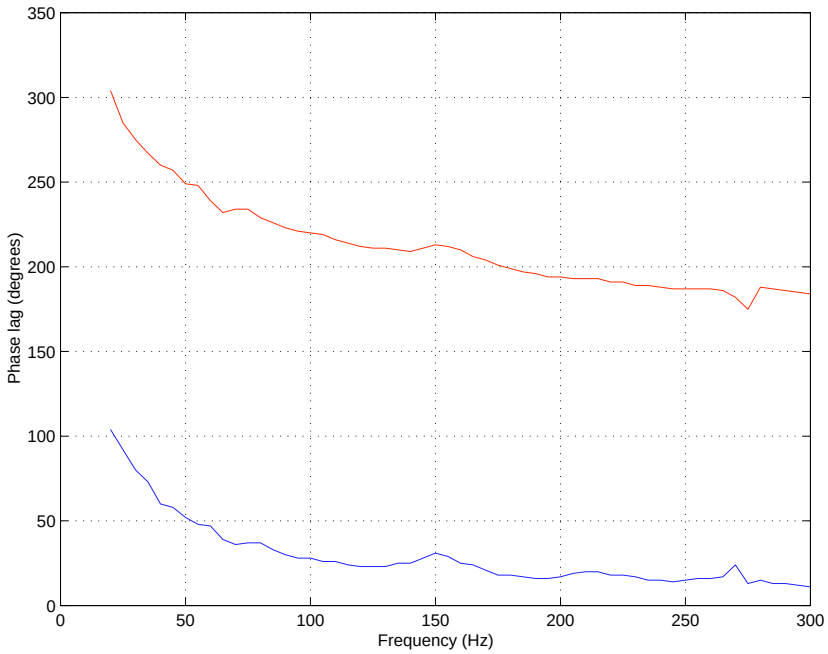

Figure 15: Phase plots of the output of the MIR when positioned 60 mm (blue) and 20 mm (red) above the target. The motion of the target is the phase reference.